2019-02-01

Explosive activity of the last 1000years at La Soufriere, St Vincent, Lesser Antilles

Cole, Paul

10.1016/j.jvolgeores.2019.01.002
Journal of Volcanology and Geothermal Research
Elsevier

Explosive activity of the last 1000 years at La Soufrière, St Vincent, Lesser Antilles

Cole, P.D.[1,*], Robertson, R.A.E[2], Fedele, L.[3], Scarpati, C.[3]

1 School of Geography, Earth and Environmental Sciences, Plymouth University, Drake Circus, Plymouth (UK)

2 UWI Seismic Research Centre, University of the West Indies, St Augustine (Trinidad and Tobago)

3 Dipartimento di Scienze della Terra, dell'Ambiente e delle Risorse (DiSTAR), Università degli Studi di Napoli Federico II - Via Cupa Nuova Cintia 21, 80126 Napoli (Italy)

* corresponding author (paul.cole@plymouth.ac.uk)

Abstract

The products of explosive activity of La Soufrière volcano on the island of St Vincent over the last 1000 years are described. Dates for the different eruptions were determined using information from contemporary accounts, fieldwork and radiocarbon dating. Scoria-flow type pyroclastic density currents (PDCs) dominate the products of both the historical eruptions (1979, 1902-03, 1812 CE) and prehistoric eruptions (~1580 and 1440 CE) with subordinate fallout components associated with several eruptions. Radiocarbon dating shows that these six eruptions define a crude cyclicity with repose periods ranging between 77 and ~140 years and systematically decreasing in more recent times.

Two prehistoric eruptions, in ~1440 and 1580 CE respectively, both produced magmatic lapilli fallout and PDCs, and were fed by slightly more evolved magmas than the historical eruptions. The eruptions in 1902 and 1812 CE had ash-rich, possible phreatomagmatic activity at their onset.

The iconic 1902-03 CE eruption generated radial distributed PDCs, which were responsible for the deaths of ~1500 people. However, only small remnants of these deposits remain and the original distribution cannot be determined from the preserved geology, which has important implications for hazard studies.

Petrochemical work has shown that magmas involved in the explosive eruptions were quite narrow in compositional range, mainly comprising basaltic andesites. The 1902-03 eruption involved a late stage basaltic component in March 1903. However, activity in the last 1000 years generated notably more homogeneous magmas with a narrower range than the older eruptive periods previously

reported in the literature, suggesting a significant variation in the magmatic reservoir feeding system with time.

Keywords: La Soufrière, St Vincent; Pyroclastic Density Currents; 1902 eruption; radiocarbon dating; Volcanic history;

1. Introduction

La Soufrière volcano on the island of St Vincent is the most active subaerial volcano in Eastern Caribbean. It last erupted in 1979, an explosive eruption that had a volcanic explosivity index (VEI) of 3 which necessitated the evacuation of 20,000 people from around the volcano. Prior to this, there have been three other historical explosive eruptions in 1718, 1812 and 1902/03. The 1902/03 eruption, of VEI 4 magnitude, which began on 7th May 1902, caused around 1500 fatalities but was somewhat overlooked in the volcanological literature, possibly owing to its occurrence the day before the catastrophic destruction of St. Pierre by Mt. Pelée in Martinique.

The four historical explosive eruptions define a weak cyclicity of explosive events occurring approximately every 77 to 94 years. Knowledge of the Prehistoric activity (prior to 1700 in the Caribbean Islands) of the volcano is limited (Robertson 2005). It is not known if this cyclicity in explosive activity is a longer-lived feature of the volcano or if it is only represented by the historical activity.

Many other volcanic systems show cycles of eruptive activity, occurring over regular time scales (e.g. Luhr and Carmichael 1990; Odbert and Wadge 2014; Lamb et al 2014). Volcan de Colima (Mexico), for example, has had at least 4 cycles, each of which has lasted around 100 years and appear to have been terminated with a powerful Plinian explosive eruption (Luhr and Carmichael 1990). Such cyclicity can provide important information regarding the behaviour of the volcanic system and defining patterns of activity is important in forecasting of potential future volcanic activity.

Forecasting becomes more difficult for volcanoes with a limited historical record (Sparks and Aspinall, 2004). Understanding the recent history of the activity of volcanoes is thus critical to assessing the volcanic hazard for the surrounding region, and this is particularly true for La Soufrière, St Vincent in what has historically been such an active volcano.

This paper addresses the gap in knowledge of the stratigraphy and petrology of the products of La Soufrière's recent history, focussing on the last 1000 years. We describe the physical volcanology of

the products formed both by the historical and recent prehistoric explosive eruptions. We use radiocarbon dating and stratigraphic studies to document these eruptions. In addition, we describe the petrology and establish the geochemistry of these products.

2. Geological setting

The island of St Vincent lies in the southern part of the Lesser Antilles (Fig. 1a), a 750 km-long intraoceanic volcanic arc developed as the result of the relatively slow (i.e., ~2-4 cm/yr; Pindell et al. 1988; DeMets et al. 2000) subduction of the Atlantic/N-American plate beneath the Caribbean plate (e.g., Macdonald et al. 2000). The island is 29 km from north to south and a maximum of 17 km from east to west (Fig. 1b) and is composed of a series of dissected volcanic centres that young from south to north, the youngest being the La Soufrière active stratovolcano. The oldest dated rocks on the island are 2.74 Ma and La Soufrière's activity began in the late Pleistocene around 0.69 Ma (Briden et al. 1979).

La Soufrière Volcano rises to a height of 1204 m (Fig.1b) and has a maximum basal diameter of 12 km from east to west. The shorter north to south diameter of 8.5 km is at least partly caused by the southern flank abutting the steep northern part of the dissected older edifice of Richmond Peak and Mt Brisbane (Fig.1c).

The summit complex of La Soufrière comprises an older Somma rim, forming the northern remnants of a 2.2 km wide caldera-type structure open to the southwest (Le Friant et al. 2009; Fournier et al., 2011). The present-day crater is nested within this caldera and is 1.5 km wide at its rim. It has a maximum depth of 370 m on its northern side and a minimum of 100 m on its western edge. A lava dome ('D' on Fig.1c) occupies the floor of the crater, is 850 m in diameter and 120 m high. It formed at the end of the 1979 eruption and continued extruding until 1980. A small, 500 m wide crater, formed in 1812, lies immediately northeast of, and cuts, the present-day crater ('1812' on Fig.1c).

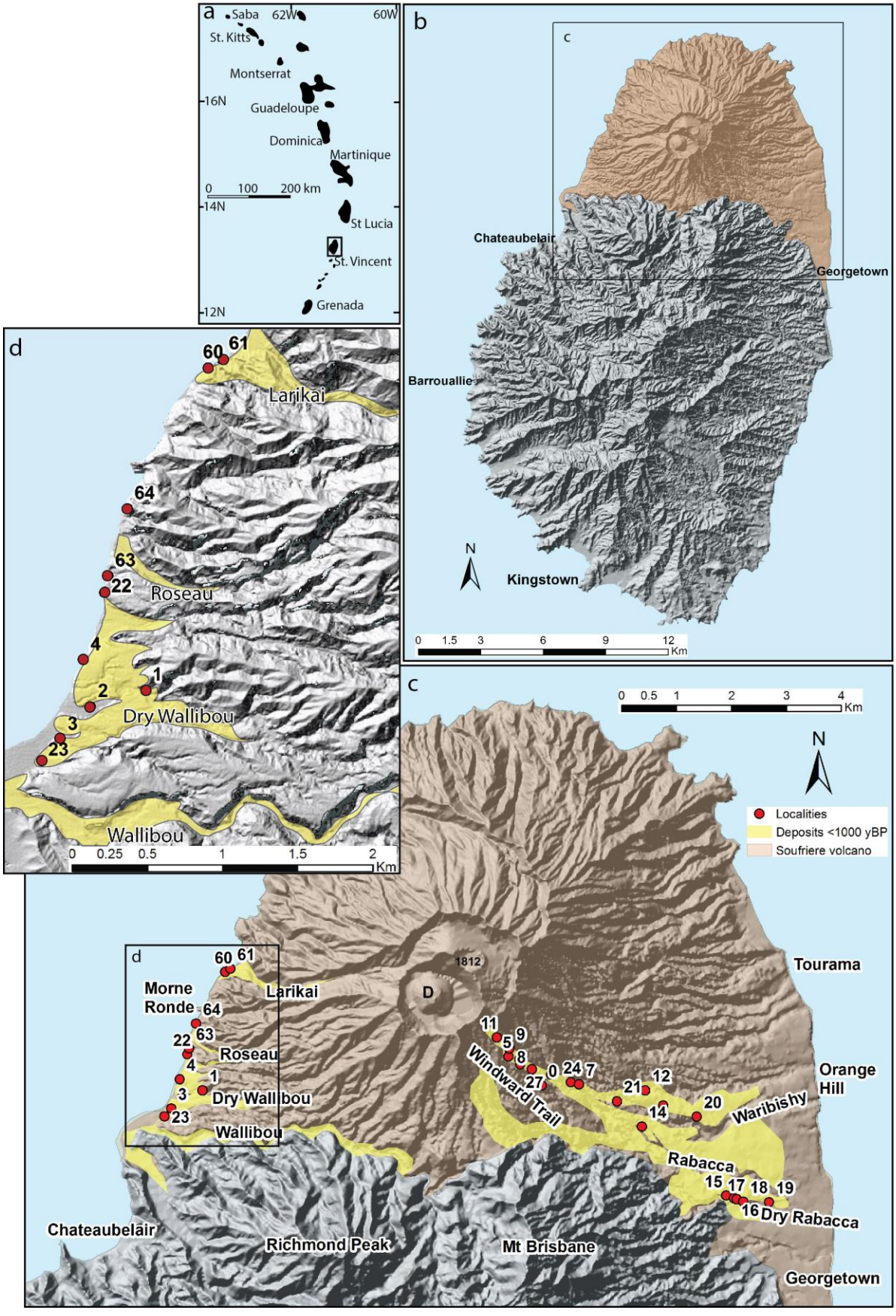
a
Saba
62W
60W
St. Kitts
Montserrat
16N
Guadeloupe
Dominica
Martinique
0 100 200 km
14N
St Lucia
St. Vincent
Grenada
12N
b
c
Chateaubelair
Georgetown
Barrouallie
N
Kingstown
0 1.5 3 6 9 12
Km
d
60 61
Larikai
64
63
22
Roseau
4
1
2
Dry Wallibou
3
23
Wallibou
0 0.25 0.5 1 1.5 2
Km
c
0 0.5 1 2 3 4
Km
N
Localities
Deposits <1000 yBP
Soufriere volcano
d
60 61
Morne
Ronde
Larikai
64
63
22
Roseau
4
1
3
Dry Wallibou
23
Wallibou
1812
D
Tourama
11
5
9
8
Windward Trail
0
24
7
27
21
12
14
20
Waribishy
Orange
Hill
Rabacca
15
17
18
19
16
Dry Rabacca
Chateaubelair
Richmond Peak
Mt Brisbane
Georgetown

Fig.1 a) Location of St Vincent in the Eastern Caribbean. b) The island of St Vincent with La Soufrière volcano shown in brown shading. c) Detail of La Soufrière volcano. Numbered localities (red dots) refer to measured sections, some of which are shown in Fig.3. Key valleys and localities mentioned in the text are also shown. D = 1979-80 lava dome. 1812 = crater formed in 1812 eruption. d) Detail of PDC deposits fans formed on the southwest coast, mostly accumulated by PDCs <1000 yr BP.

Knowledge of the prehistoric activity of La Soufrière is scant. The lowermost flanks are composed of basaltic lavas, considered part of the prehistoric Somma volcano and are dated between 0.36 and 0.69 Ma (Briden et al., 1979). A Yellow pumiceous tephra (Yellow Tuff Formation) containing several topography-mantling lapilli fallout layers, that can be traced across the northern part of the island (Rowley 1978b), overlie these lavas. Overlying this Yellow Tuff Formation on the lower flanks of La Soufrière, are alluvial deposits and lahars interbedded with the deposits of primary pyroclastic density currents (PDCs) (Robertson 2005). St. Vincent has also had effusive eruptions; such as in 1971, when a lava dome was erupted over a period of 4 months (Aspinall et al. 1973; Shepherd et al. 1979; Graham and Thirlwall 1981).

3. Contemporary accounts of the historical explosive eruptions

3.1 1718 CE

There is little geological or volcanological information related to the 1718 eruption from contemporary documents. Dafoe (1718) describes tephra fallout up to approximately 30 cm in thickness which occurred on ships in the region and also on several other Caribbean islands, including Martinique (up to approx. 20 cm of tephra) as well as on Barbados, St Kitts, and possibly the Dominican Republic (Anderson and Flett, 1903). Solely the native Caribs populated the island at this time. There is however no information relating to the products on the island or any evidence of resulting fatalities, athough (Dafoe 1718) states that incandescence was observed from ships. Thus the evidence indicates there was a not inconsiderable explosive eruption at this time.

A steaming dome was present in the crater in 1784 (Anderson and Yonge 1785) which has been used to speculate on the possibly effusive eruption at this time.

3.2 1812 CE

The eruption began at midday on 27th April, after a series of more than 200 earthquakes were reported over the previous year (various contemporary newspapers). Semi-continuous tephra fallout occurred for three days until 30th April when, associated with apparently continuous tremor, the eruption intensified. The following account of part of the eruption is of note (Blue Book 1902) *'…and scaling every obstacle, carrying rocks and woods together in its course down the slope of the mountain, until it precipitated itself down some vast ravine, concealed from our sight by the intervening ridges of Morne Ronde. Vast globular bodies of fire were seen projected from the fiery furnace, and bursting, fell back into it, or over it on the surrounding bushes, which were instantly set in flames. About four hours from the lava boiling over the crater it reached the sea, as we could observe from the reflection of the fire and the electric flashes attending it. About half-past one another stream of lava was seen descending to the eastward towards Rabaka.'* Furthermore, as a number of these accounts (e.g. Shepherd, 1831) refer to 'lava emissions' it seems likely that these phenomena involved hot material. While these could be lahars, the death of 50 people, as well as extensive cattle and human fatalities in the Wallibou region to the southwest, indicate that these were PDCs (Shepherd, 1831; Smith, 2011).

Tephra fallout associated with the 1812 eruption continued for several days significantly affecting the eastern side of the island (Carib territory). Reports (Shepherd 1831) indicate 10 -20cm of tephra fallout in several regions on the eastern flanks of the volcano. Ashfall also occurred for 18 hours in Barbados (Smith 2011).

3.3 1902-03 CE

The 1902-03 eruption was extraordinarily well-documented in a series of contemporary accounts including the detailed documents of Tempest Anderson and co-workers (e.g. Anderson and Flett 1903, Hovey 1903, Anderson 1908). These documents provide a rich record of the products of this eruption and its impact on the island. There were three main phases: the first on 6th May, another in September and October 1902 and the final phase in March 1903. The eruption began on 6th May 1902 after around 13 months of precursory felt seismicity. A crater lake existed prior to the eruption and initial activity comprised a series of explosions with considerable steam involvement. The first observations of incandescence at the crater were made during the evening of 6th May. Estimates from contemporary sources indicate that eruption columns, associated with some of the initial precursory explosions, reached > 1 km above the crater rim.

Tephra fallout started around 11 am on the morning of 7th May with fine ash fall, and an increase in the calibre of fallout was reported, with lapilli sized fallout being reported on the south eastern side of the volcano, in the Orange hill region, at around 12 pm.

At around 2pm on 7th May the paroxysmal phase of the eruption occurred with the formation of what was initially termed the 'great black cloud' by Anderson and Flett (1903). These descriptions relate to the formation of an extensive PDC, which travelled down nearly all flanks of the volcano, resulting in more than 1500 fatalities (Pyle et al., 2018). This PDC reached the coastline in a number of places and continued across the sea for several kilometres.

Further significant explosive activity occurred between 13 and 14 October 1902, and 21 and 30 March 1903 (Anderson 1908). Activity both in October 1902 and in March 1903 accumulated deposits confined at base of the Larikai valley (Anderson 1908 p290 and 295) which are likely to have been formed by PDCs. Extensive tephra fallout occurred associated with both events, in October 1902 up to 20 cm of scoria fallout was reported on the coast to the east of the volcano. Black, vesicular lapilli deposit, up to 12.5 cm thick, were observed in Tourama, on the eastern flank, in March 1903. Significant tephra fallout also occurred in Barbados associated with both these events (Anderson 1908).

3.4 1979

The 1979 eruption began suddenly on the 13 April following elevated seismicity. The explosive phase, consisting of a series of 11 Vulcanian type explosions, occurred over 13 days until 26th April. Eruption columns developed from a number of these explosions reached 18 km above sea level (Brazier et al 1982). The explosion on 17th April generated radial 'base surge type' PDCs to a distance of 2 km from the crater (Shepherd and Sigurdsson 1982). Minor, completely valley confined, PDCs descended the Larikai valley reaching the sea to the west, as well as the Roseau valley to the southwest and part way down the Rabacca valley to the southeast (Shepherd et al. 1979). Ashfall occurred extensively across the island and on the island of Barbados.

4. Radiocarbon dating

To relate the exposed products on the flanks of the volcano to specific eruptions, samples of charcoal were collected and radiocarbon dated from a range of primary PDC deposits that represent the youngest deposits formed in the volcano recent history.

Previously, Robertson (2005) listed eighty-one radiocarbon dates from this volcano, compiled from three unpublished PhD and MPhil theses (Rowley 1978a, Robertson 1992 and Heath 1997), mostly with limited stratigraphic information. These dates show distinct clusters, one comprising 53 dates that range from ~ 600 yr BP to present day, whereas a second older cluster of 25 dates mainly from the southeast and eastern flanks range from ~2000 to 5000 years. The radiocarbon dates of Hay (1959) from the Rabacca valley at 3,800 ±300 and 4,090 ±50 yr BP correspond to this older range.

Our new radiocarbon dates are presented graphically in Figure 2 (with details in Table 1), and mostly correspond to the earlier period, younger than 600 yr BP to present day. As all charcoal samples except one were collected from primary pyroclastic deposits, we assume that these record the date of the eruption that formed them. One sample (C8 Fig. 2 and Table 1) was a charcoal fragment embedded in a palaeosol which is situated below the 1580 CE pyroclastic deposits on the Windward Trail, approximately 1 km SE of the crater rim. Three pre-existing dates from Robertson (1992) were also included in Fig.2 and Table 1 where, owing to stratigraphic information, we can be confident that they relate to the deposits studied here.

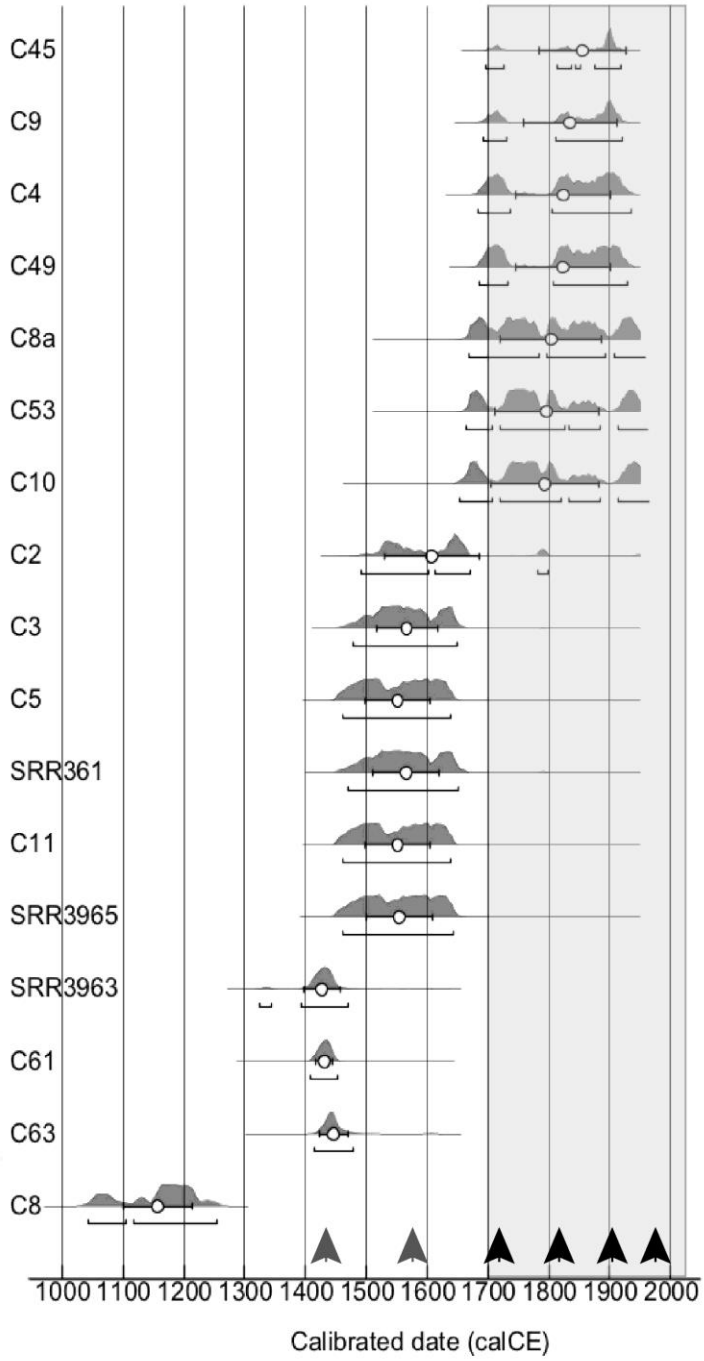

196

197 **Fig 2** Calibrated radiocarbon dates used in this study. Plots are made using the Oxcal program
198 version 4.3.2 (Bronk Ramsey 2009) using the IntCal13 Atmospheric curve. 95.4% confidence ranges
199 are shown and median ages (open circles). The grey shaded zone relates to the historic period of St
200 Vincent >1700 CE. Arrowheads show the timing of the six eruptions identified. For details of
201 radiocarbon dates see Table 1

202

203

Sample	Pre-treat	Conventional date (BP)	95.4% (1⍰) Cal age range AD and relative area	Most probable Date CE	Stratigraphic unit
C45	acid/alkali /acid	**20 ± 30**	1696 – 1726 17% 1813 – 1837 12% 1844 – 1852 2% **1876 – 1919 65%**	1902***	Uppermost PDC deposit of 3 PDCs in Dry Wallibou
C4		**79 ± 37**	1682-1736 26.2% **1805-1935 69%**	1812,	Second deposit of 3 PDC deposits in Dry Wallibou
C49	acid/alkali /acid	**90 ± 30**	1685– 1733 26% **1796– 1928 69%**	1812, 1902 1718	Uppermost thick (10m) unit on Wallibou coast
C8a		**146 ± 35**	**1667-1783 45%** 1725-1892 33% 1908 – pres 17%	1718 1812	Proximal SE flank Uppermost PDC deposit
C53	acid/alkali /acid	**160± 30**	1664 -1707 19% **1719- 1826 47%** 1832 - 1884 13% 1914 – pres 19%	1812 1718	Windward trail SE flank 1 km from crater
C10		**172 ± 37**	1654-1707 19% **1719-1820 48%** 1832-1883 11% 1914-pres 19%	1812 1718	Proximal SE flank
C2		**273 ± 35**	**1491 – 1603 50%** 1614- 1670 39% 1781-1799 6%	1560	Charcoal from thick PDC deposit midway up Dry Wallibou valley
C3		**313 ± 35**	1477 – 1650 95.4%	1566	Third deposit of 3 PDC deposits in Dry Wallibou
SRR 3961*		**315 ± 40**	1471 – 1651 95.4%	1553	PDC deposits in Wallibou sea cliff
SRR 3965*		**340 ± 40**	1462-1642 95.4%	1580	Larikai sea cliff section midway up
C5		**347 ± 35**	1460-1638 95.4%	1590	SW coast lowest PDC deposit fallout at base
C11		**347 ± 35**	1460 -1638 95.4%	1551	Proximal SE flank, charcoal from coarse, fines free lapilli deposit
SRR 3963*		**485 ± 40**	1393 – 1470 95.4%	1426	Larikai sea cliff section lowermost unit.
C63	acid/ alkali/acid	**450 ± 30**	1415 -1479 95.4%	1445	Larikai sea cliff section lowermost BAF deposit
C61	acid/ alkali/acid	**480 ± 30**	1408-1452 95.4%	1430	Larikai sea cliff section Lowermost Scoria flow deposit
C8		**870 ± 37**	1043-1104 22% **1118-1254 73%**	1157	Large single charcoal fragment in soil on Windward Trail

204

205 **Table 1** Radiocarbon dates - the three dates SRR361, 3965 and 3963 are from Robertson (1992).
206 Dates have been calibrated using the OXCAL version 4.3.2 program (Bronk Ramsey et al. 2009). All

samples were analysed by AMS (Accelerated mass Spectrometry.) Numbers in bold are the most probable dates based on the calibration statistics.

Historical time, the date when Europeans colonised the Eastern Caribbean region, is from 1700 CE onwards. As discussed earlier, there were four explosive eruptions in historical time while, prior to this, there are no written accounts from the native Carib population that inhabited St Vincent.

The majority of radiocarbon dates fall into two broad groups, with little or no overlap between them: a group relating to historical period (shaded grey on Fig.2), and a second group within prehistoric time. The lack of overlap in the uncertainties between the historic and prehistoric groups of dates indicates that the prehistoric ages represent distinct eruptions.

Radiocarbon dates from the period of the historical explosive eruptions: 1718, 1812 and 1902 are associated with a large uncertainty related to carbon release from burning of fossil fuels since the industrial revolution, therefore diluting radioactive carbon-14. As a consequence, the calibration of dates <300 yr BP makes it difficult to determine which of the three major historical eruptions these dates are associated with (Table 1 and Fig.2).

We further subdivided the prehistoric radiocarbon dates into two age groups: those occurring in the 16th Century (C2, C3, SRR3961, SRR3965, C5 and C11) and those in the mid-15th century (SRR3963, C63 and C61). The 16th Century dates have uncertainties ranging from 1485 to the early 1640 CE (Table 1 and Fig. 2). However, the 15th Century dates have narrower uncertainties ranging across only 38 years from 1414 to 1452 CE (for 3 radiocarbon dates), with very little overlap in uncertainties between the 15th and 16th Century group of dates (Fig. 2). Analysis shows that these two groups statistically represent distinct dates (Stuiver et al 2018). Moreover, we used the 'Combine' function of the OxCal v 4.3.2 program to determine model calibrated ages of the two groups, which give a 95.4% confidence limit of 1494 - 1632 CE for the 16th Century eruption and 1421 -1448 CE for the 15th century eruption.

To summarise this evidence strongly indicates that there were at least two prehistoric eruptions in the last 600 years, one occurring in the mid-15th Century (mean age 1440 CE) and another occurring in the later 16th Century (mean age 1580 CE).

The charcoal sample C8 with a calibrated age range between 1043 and 1254 yBP from a thick palaeosol below the other eruptions described here indicates that there was a longer repose period of at least 250 years and possibly much longer, prior to the 1440 yBP event.

Below we describe the products of the major historic eruptions, identified at least partly from radiocarbon dating, and those related to the two prehistoric eruptions constrained at around 1580 CE and 1440 CE, respectively.

5. Stratigraphy and products

Measured sections at more than fifty localities on the south-western and south-eastern flanks were documented during the course of this study (selected sections are shown in Figs. 1 and 3). These exposures occur in and around drainages that extend from the southern part of the summit crater.

Valley confined PDCs associated with eruptions in the last 1000 years were strongly controlled by the pre-existing crater and Somma rim, and apparently moved down the southern flanks. Consequently, only the south-western and south-eastern flanks preserve a record of this activity (Fig.1c). Even when PDCs spread radially around the volcano, as during the 1902 eruption, deposits are not preserved in these regions, probably due to their thin and unconsolidated nature meaning they were rapidly eroded.

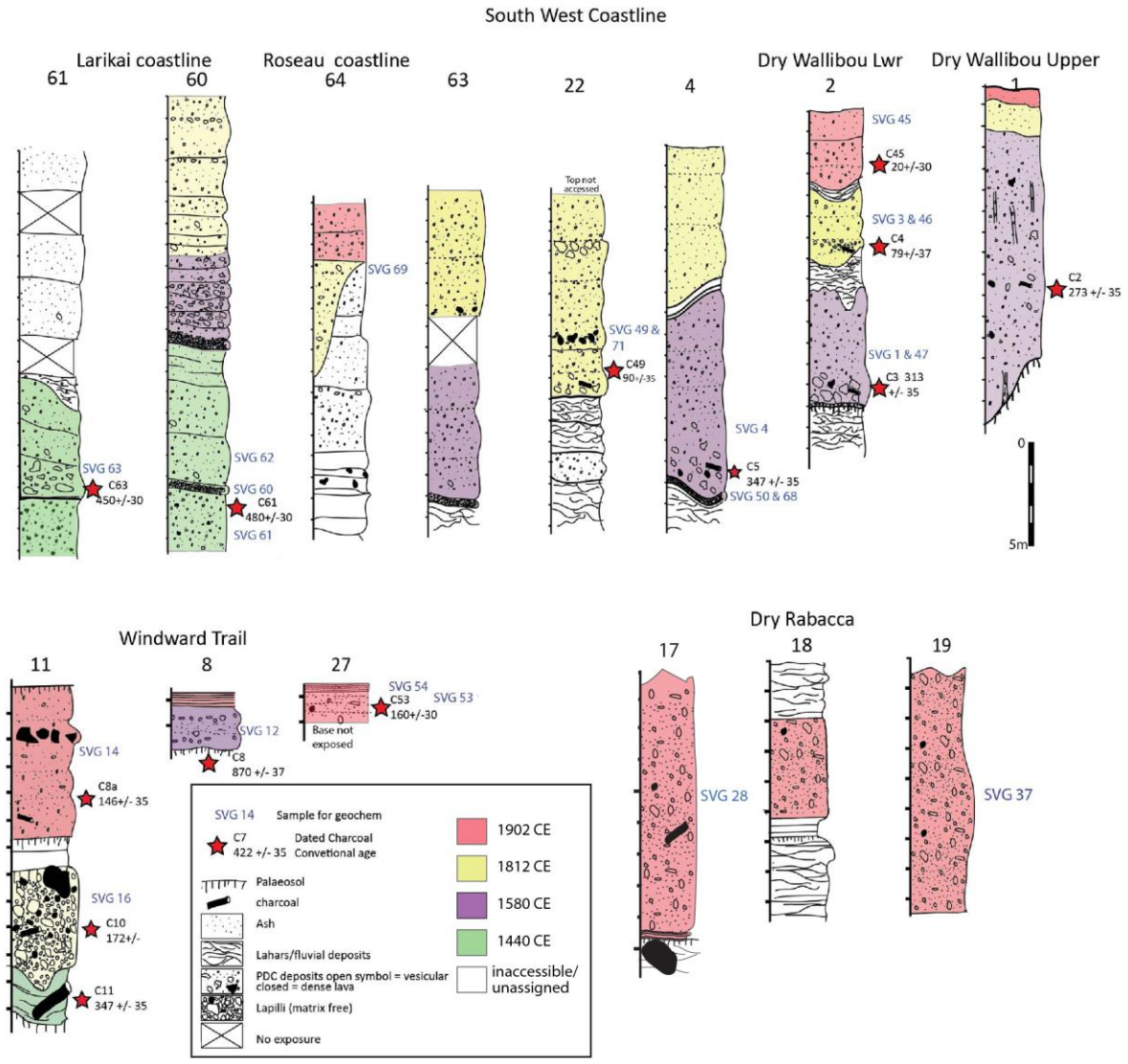

Fig 3 Selected measured sections from the flanks of the volcano. Blue letters refer to samples analysed for geochemistry. Red stars indicate charcoal samples for radiocarbon dating (only conventional dates are shown - for details see Table 1 and Fig.2). Numbers at top of sections refer to locations shown in Fig.1.

On the south-western side, valleys containing exposures of pyroclastic and volcaniclastic deposits include, from north to south, the Larikai (which drains the lowermost part of the crater rim), Roseau, Dry Wallibou and Wallibou river valleys, whereas on the south-eastern side the Rabacca and Dry Rabacca valleys drain directly from the crater (Fig.1c). Pyroclastic and volcaniclastic material erupted in the last 1000 years has formed a series of fans within and at the mouths of the valleys draining the southern part of the crater (Figs 1c and d).

La Soufrière's recent history is dominated by scoria-rich pyroclastic density currents, with subordinate deposits of both ash and lapilli fallout (Robertson 2005). Interbedded between the primary pyroclastic products, are water-reworked deposits such as lahars.

Deposits of the smaller 1979 explosive eruption have been nearly completely removed by erosion and as a consequence the scattered remnants were not considered in this study.

6. Volcanic products

Each eruptive unit is described on the basis of its lithological and textural features. Grain-size and component analyses of selected unconsolidated deposits were carried out in order to provide further insight into the nature of the deposits. Although petrology and geochemistry are dealt with later in a separate section, some simple geochemical trends (SiO_2) are described here to evaluate possible compositional variations within eruptions. Interpretation of the eruptive and transport mechanisms are suggested for each eruptive unit.

6.1 1440 CE deposits

These products were identified immediately south of the Larikai valley, which drains the lowest point of the crater of La Soufrière, where a ~30 m thick sequence is exposed, representing a number of eruptions (Fig.3 - section 60 and 61). Other exposures of this deposit occur in the upper part of the 'WIndward trail' on the south east flank (Fig.1).

At Larikai the lowermost part of the sequence is formed by > 4 m of massive, poorly-sorted deposit, rich in dark grey to mauve feldspar-phyric scoria clasts that are notably poorly vesicular (unit 61, Fig 4a). These dense, scoria clasts are up to 35 cm across, although typical sizes are around 10 cm. The scoria deposit is overlain by a coarse-grained, well-sorted lapilli layer that is up to 45 cm thick (Figs 3 section 60 and 61 and unit 60, Fig.4a). The lowermost part comprises thin cm scale, fine-grained lapilli and interbedded ash layers (< 2 cm) showing notable lateral thickness variations. The main part (uppermost 30 cm) of the lapilli displays reverse to normal grading, and is composed predominantly of dense, poorly-vesicular juvenile clasts and abundant dense lava fragments. Vesicular scoria form only 18 wt% of clasts > 2 mm (unit 60, Fig.4a). Erosively overlying this lapilli several reverse graded, scoria-rich beds, up to 1.5 m thick, form a 5 m thick sequence (unit 61, Fig 4a). Each bed comprises poorly sorted, ash-rich deposit containing dark grey to black, plagioclase-phyric vesicular scoria clasts up to 50 cm across. There are no significant variations in SiO_2 between

different parts of the same eruptive unit (Fig.4a).

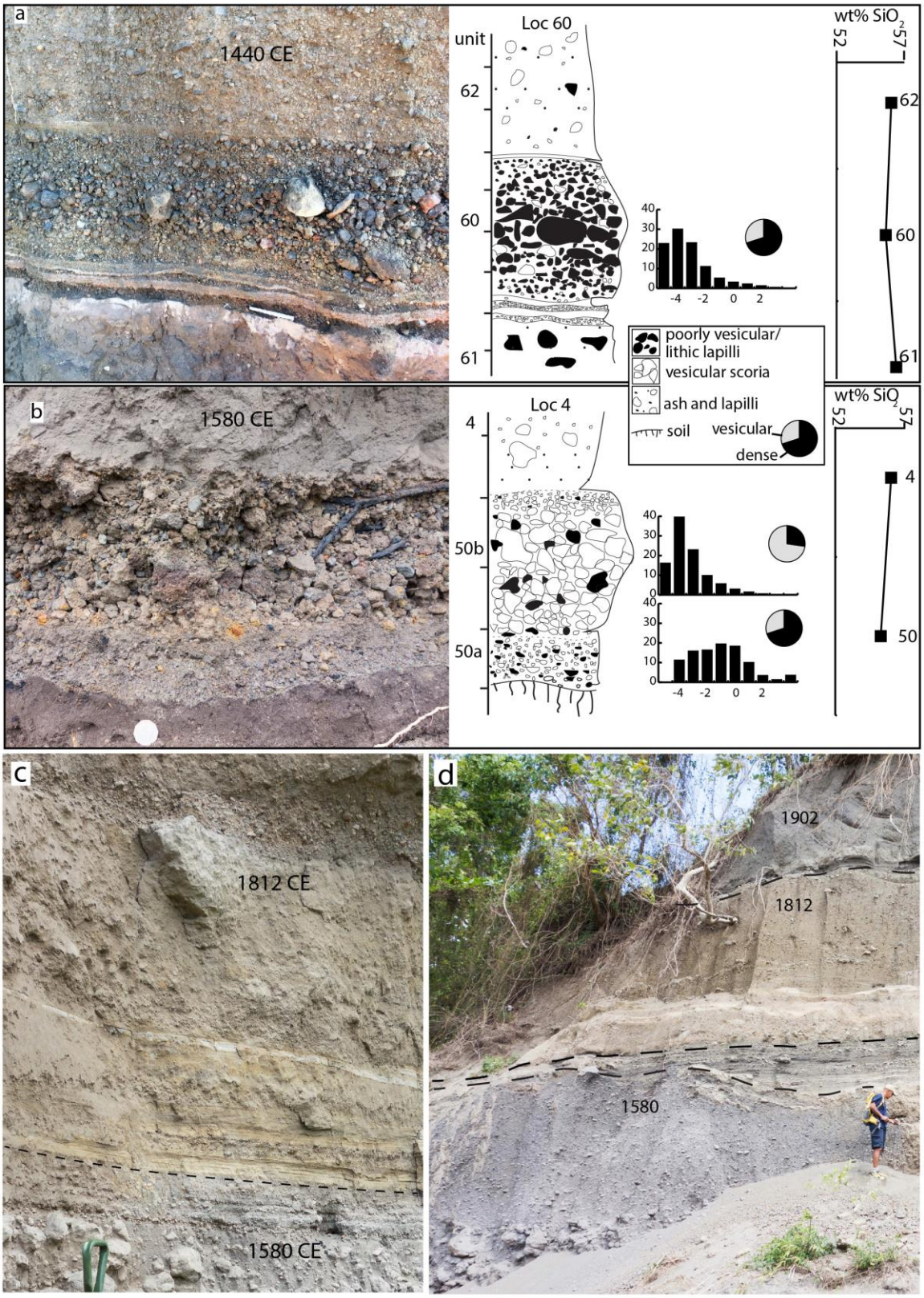

Fig 4 a) Sequence associated with the 1440 CE eruption, immediately south of the Larikai valley (Loc 60 on Fig 1). At the base: poorly-sorted, scoria deposit; middle: lapilli fallout layer; top: reverse

graded, scoria-rich beds. Grainsize histograms and pie charts show components >2mm in size, grey= vesicular scoria, black = dense lava. On the right is also shown the SiO_2 variation with stratigraphic height. b) Lapilli fallout resting on the palaeosol at the base of the 1580 CE deposits(Loc 4 on Fig.1). The lapilli deposit is overlain by a massive, poorly sorted, scoria-rich deposit. Grainsize histograms are shown. Piie charts show components >2mm in size. On the right is also shown the SiO_2 variation with stratigraphic height. c) Basal 2 m of 1812 CE deposits in the Dry Wallibou valley (near Loc 2 on Figs. 1 and 3). Thin ash layers are interbedded with thin coarser, massive poorly sorted layers and cross-bedded deposits. Deposits sit atop 1580 CE PDCs. d) Sequence of three PDC deposits exposed in the northern wall of the Dry Wallibou valley on the southwest flank (Loc 2 on Figs.1 and 3). The uppermost deposit is interpreted as 7th May 1902 PDC deposit, with 1812 CE and 1580 CE below. Dashed lines enclose lahars and fluvial deposits interbedded between the primary eruptive units.

Owing to the presence of abundant poorly vesicular juvenile material, we interpret the lowermost units of this sequence as 'block and ash flow type PDCs', possibly relating to lava dome collapses in the crater. The lapilli layer is interpreted as fallout from a considerable eruption column and the beds in the uppermost part are scoriaceous PDC deposits typical of St Vincent's recent activity, derived from eruption column collapse.

6.2 1580 CE deposits

These products form some of the lowermost primary pyroclastic deposits around the Wallibou and Dry Wallibou valleys and the coastal exposures between them (Fig.3 sections 1-4) and overlie fluviatile reworked volcaniclastic deposits. Up to 30 cm of distinctive well-sorted scoria lapilli form the lowermost part (units 50 a and b, Fig.4b). This lapilli unit is composed of a lower finer grained, 8 cm thick part that is notably poor (30 wt% > 2 mm) in vesicular scoria (50a) and an upper, coarser, normally graded, 22 cm thick unit containing abundant (72 wt% > 2 mm), highly-vesicular, pale grey scoria clasts (unit 50b, Fig 4b). Subordinate dense lava and hydrothermally altered lithic clasts are also present within this lapilli layer.

Massive, poorly sorted, scoria-rich deposits overlie the lapilli layer (unit 4, Fig 4b). These are locally > 30 m thick in the lower reaches of the Dry Wallibou valley on the SW flank, forming the thickest deposits of this unit. More typically these massive deposits are ~5 m thick in continuous sections (> 100 m long) on the southwest coast (Fig. 3, sections 1-4). Although generally massive and structureless, in some sections a number of subunits can be recognised ranging between 1 and 3m in thickness, defined by distinct changes in grainsize. Abundant fragments of carbonised wood occur within these deposits. Accumulations of abundant, coarse (up to 70 cm in diameter), dark grey to black vesicular scoria clasts are locally present at the base of these massive deposits, forming discontinuous normal grading (Fig. 4 d). The basal lapilli layer is composed of slightly less evolved

(55.5 wt.% SiO_2) scoria than the overlying scoria-rich deposits (56.3 wt.% SiO_2) of the same eruption although the differences are probably not significant (Fig. 4b) as all the other major and trace elements are remarkably homogeneous (see “Petrology of the scoria clasts” section).

The basal lapilli layer is considered the product of fallout from a convecting eruption column at the start of the eruption with the progression from a finer scoria-poor part (unit 50a, Fig 4b) to higher column that generated the coarse scoria-rich phase (50b, Fig 4b). This lapilli layer is not present at the base of all localities (see sec 1 Fig.3), presumably owing to erosion either by the later PDCs or between phases of the same eruption. The overlying massive, poorly sorted deposits are interpreted as the products of PDCs. Such an interpretation is supported by the abundance of charcoal, local accumulations of coarse scoria clasts and large thicknesses variations observed. These latter were probably related to valley filling of the PDCs in the deep ravines that extend from the crater, such as the Dry Wallibou valley.

6.3 1718-1812 CE deposits

The lack of almost any contemporary information on the 1718 eruptions, coupled with an absence of distinctive field characteristics and large uncertainty in radiocarbon ages makes the distinction of the products of the 1718 and 1812 eruptions difficult.

Nevertheless, contemporary accounts of the 1812 eruption (described earlier) clearly indicate that PDCs moved down a number of valleys to the west, southwest and south-eastern flanks of the volcano. In the southwest, along the Dry Wallibou valley (Fig. 3), pyroclastic deposits underlying the 1902 products and on top of 1580 CE deposits (Fig. 4d) are lighter in colour and contain paler, pumiceous material. In addition, they are generally finer-grained than overlying and underlying deposits, containing only rare scoria clasts > 10 cm in diameter.

The basal part of this sequence contains a number of thin, 1-2cm thick, ash layers (Fig.4c). Several layers display cross-bedding and are interbedded with thin <15 cm massive, poorly sorted deposits. The upper part of this pyroclastic sequence is composed of 3 - 6m thick, poorly sorted, massive, valley ponding deposits.

The lowermost ash-rich layers are interpreted as having been formed by fallout. The fact that ash fall out dominated the first three days of the 1812 eruption suggest that these deposits relate to this event. A radiocarbon date of charcoal from these deposits indicates that there is a 69% probability that the age range is between 1805 and 1935 CE. As 1902-03 deposits overly this unit, we therefore consider these deposits to be products of the 1812 eruption.

We suggest that the cross-bedded and thin massive deposits may be the product of low concentration PDC, whereas the more massive units formed from higher concentration currents.

6.3 1902-03 CE deposits

Remnants of the products of the 1902-03 deposits are identifiable mainly on the southeast and southwest flanks of the volcano (Fig. 3). In the Dry Rabacca valley to the southeast a basal tephra sequence, up to 20 cm thick, overlies coarse-grained fluviatile deposits (Fig. 3 section 18 and Fig. 5a). The basal tephra sequence is composed of several mainly fine grained, ash-rich layers. A distinctive 2 cm thick, orange, fine lapilli layer occurs 2 cm above the base (unit 2, Fig 5a) , dominated by abundant hydrothermally altered fragments. This is overlain by a 10 cm thick, ash-rich, accretionary lapilli-bearing layer (unit 3, Fig 5a) that grades upwards into a coarser, diffuse vesicular scoria lapilli, containing clasts up to 2 cm in diameter (unit4, Fig 5a). To the southwest the basal sequence is either absent or locally present as 1 -2 cm of fine ash. Component analyses show that vesicular juvenile scoria in varying quantities is a ubiquitous component throughout this sequence. Although lithic material composed of both dense lavas and hydrothermally altered fragments form > 50% of clasts (>2 mm) in a number of layers (Fig. 5a).

On the south-western side of the volcano, in the Dry Wallibou valley, the lowermost 1902 products comprise up to 30 cm of dune bedded deposits that sit erosively on older (1718/1812 CE) pyroclastic products (Fig. 4d). A massive, poorly sorted, indurated deposit, up to 28 cm thick, overlies this which is in turn overlain by unconsolidated, massive, poorly sorted, scoria-rich deposits up to 5 m thick (Fig. 3 Section 2).

On the south-eastern flank, sections through 1902-03 products (Dry Rabacca valley) comprise thick, > 20 m, massive, coarse-grained, poorly sorted scoria-rich deposits (Figs. 3 and 5b) overlying the basal tephra sequence. These deposits are structureless without stratification, although there is some slight coarsening within the central part (Fig. 5b). On ridges and topographic highs on the south-eastern flank in the region between Orange Hill and the Windward trail region (around 1 – 4 km from the crater) the uppermost 1902-03 deposits are formed by a distinctive sequence (Fig. 5c). Poorly sorted, stratified deposits (unit 24, Fig 5c) up 60 cm thick, containing thin, discontinuous lenses of fine lapilli, form the base of the sequence and rest on a weakly developed palaeosol (not shown in Fig 5c). Locally a 5cm thick, fine grained, accretionary lapilli bearing ash layer caps this unit (unit 24a, Fig 5c). A 12 cm thick grey, well-sorted lapilli layer overlies this (unit 43, Fig 5c) , although outsized vesicular scoria blocks form ballistic impact structures, and is capped by up to 2 cm of fine

ash (unit 43a, Fig 5c). The uppermost unit is a distinctive dark, well-sorted lapilli layer, up to 40 cm in thickness, composed almost entirely of vesicular purple to black scoria lapilli (unit 42, Fig 5c). Dense (lithic) lava fragments are notably rare to absent from this layer. Geochemical analyses show that the lower stratified deposits contain basaltic andesite scoria with 54 wt.% SiO_2, whereas the uppermost lapilli fallout is basaltic in composition, 50-51 wt.% SiO_2 (Fig.5 c).

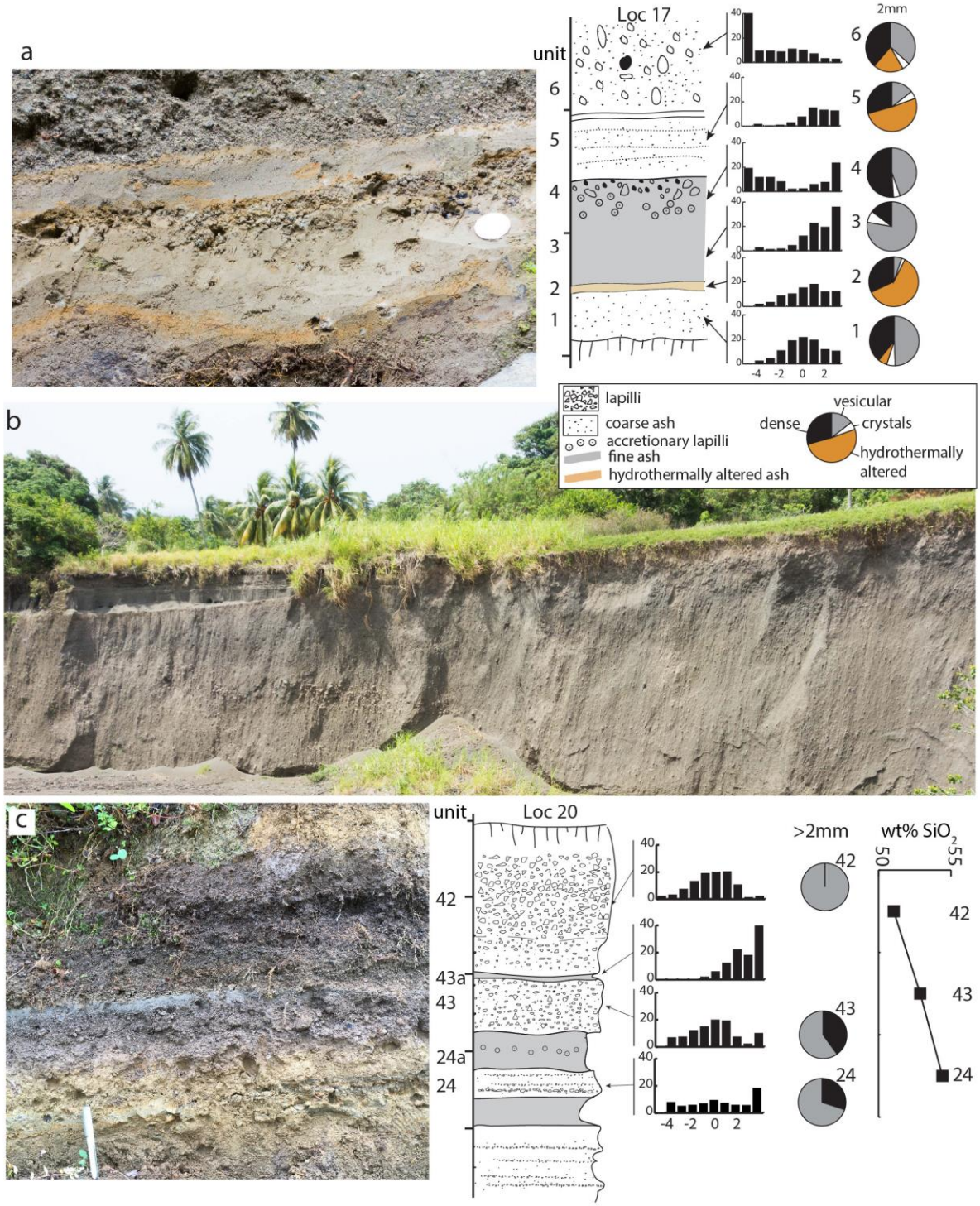

Fig 5 a) Basal part of 7th May 1902 fallout sequence, exposed in the Dry Rabacca valley (near Loc 17 on Fig.1). b) Massive 7th May 1902 PDC deposits exposed in the Dry Rabacca valley (Loc 19 on Fig.1). c) Stratified 7th May 1902 PDC deposits (orange), overlain by pinkish lapilli and a thin ash and dark brown scoria-rich lapilli fallout layers thought to be formed by October 1902 and March 1903 activity, respectively. Photo of the described stratigraphic sequence (on the left) with representative measured section (Loc 20 on Fig.1). Grainsize histograms and component pie charts depict components >2 mm in size: grey = vesicular scoria, black = dense lava; orange = hydrothermally altered lithic material. On the right is also shown the SiO_2 variation with stratigraphic height.

The basal tephra sequence in the Dry Rabacca valley is interpreted to have been formed by fallout during the initial phase of activity in the late morning of 7th May 1902. Within this sequence the coarser scoria lapilli horizon, within otherwise ash-rich material, is considered to represent fallout from magmatic, Vulcanian style, explosions and possible correlates with an increase in calibre of fallout described in contemporary documents that occurred at 12 pm on 7th May (Anderson and Flett 1903). The presence of vesicular scoria clasts throughout the sequence indicate widespread fragmentation of gas-rich magma from the onset of eruptive activity. However, the abundance of hydrothermally altered lithic clasts (which dominate some layers) and accretionary lapilli suggests that phreatomagmatic activity generated some of these ash layers.

We interpret the massive deposits of the upper part of the sequence to have accumulated from high concentration PDCs that were clearly valley confined and formed during the paroxysmal phase of the eruption on the afternoon of 7 May 1902. Moreover, contemporary reports, from field studies, in the weeks immediately after the eruption, described a ‘glacier like’ deposit within and blocking the Rabacca valley (see Plate39 Fig.1 of Hovey 1903), that is now referred to as the Dry Rabacca valley. Massive deposits exposed in walls of this valley are considered the dissected remnants of this ‘glacier like’ PDC deposit (Fig. 2 and 5 b).

In the Dry Wallibou, on the SW side, dune bedded deposits represent initial dilute PDCs with the indurated massive deposit possibly representing a lahar formed contemporaneously with the initial PDCs.

The thin, crudely stratified, poorly sorted deposits confined on the ridges are interpreted as products of low particle concentration PDCs, related to the paroxysmal phase, on the afternoon of 7th May 1902 that swept radially away from the crater. The grey intermediate lapilli layer is interpreted to represent fallout from October 1902 activity and the uppermost lithic-free, scoria lapilli fallout layer was formed by explosive activity in March 1903. Such an interpretation is supported by the basaltic composition of these lapilli as Roobol and Smith (1975) showed that the products of the March 1903 eruption were basaltic.

7. Petrology of the scoria clasts

Thirty single scoria samples belonging to the investigated La Soufrière eruptions were collected and then processed for petrochemical characterization at the DiSTAR laboratories (Napoli, Italy). Samples were crushed, washed in deionized water, dried out and pulverized in a low-blank agate mill. Rock powders were analysed by ICP-OES (Inductively-Coupled Optical Emission Spectrometry) and ICP-MS (Inductively-Coupled Plasma Mass Spectrometry) for major- and trace elements and weight loss on ignition (LOI) at ActLabs (Ontario, Canada). Samples were mixed with a flux of lithium metaborate and lithium tetraborate, and fused in an induction furnace. The melts were poured into a solution of 5% nitric acid containing an internal standard and mixed continuously until completely dissolved (~30 minutes). The samples were analysed for major oxides and selected trace elements (Ba, Be, Sc, Sr, V, Y and Zr) by Thermo Jarrell-Ash ENVIRO II or a Varian Vista 735 ICP optical spectrometer. Calibration was performed using USGS and CANMET certified reference materials. Fused samples were diluted and analysed by Perkin Elmer Sciex ELAN 6000, 6100 or 9000 ICP-MS for other trace elements. See www.actlabs.com for full analytical details.

The composition of the main mineral and glass phases was analysed for a selection of 10 representative samples by EDS (energy dispersive spectrometry) at the DiSTAR (Napoli), using an Oxford Instruments Microanalysis Unit equipped with an INCA X-act detector and a JEOL JSM-5310 microscope. Measurements were performed with an INCA X-stream pulse processor using a 15 kV primary beam voltage, 50-100 μA filament current, variable spot sizes and 50 seconds of acquisition time. Relative analytical uncertainty is typically ~1-2% for major elements, ~3-5% for minor elements. The results of all the petrological analyses are reported in the Electronic Supplementary Material 1.

7.1 Petrography

All juvenile scoria samples are strongly to moderately porphyritic (locally glomeroporphyritic) with abundant plagioclase and clinopyroxene phenocrysts, together with less abundant olivine and/or orthopyroxene, set in a weakly to moderately vesicular glassy groundmass. All the main crystal phases typically contain inclusions of glass and other mineral phases (SMFig. 1). Numerous types of enclaves (mostly holocrystalline, ranging from gabbroic to ultramafic) are also observed, a feature that is extremely common for the juvenile products of the entire activity of the La Soufrière volcano (e.g., Heath et al. 1998; Tollan et al. 2012). Although generally similar, some small significant differences occur between samples from different stratigraphic units (Table 2).

Scoria from the 1902-03 eruptions shows the widest petrographic variability with two different types present. The most common scoria type is dominated by large plagioclase phenocrysts (up to 2 mm in length) with generally smaller colourless to pale green clinopyroxene, colourless to pale yellow orthopyroxene and few olivine phenocrysts/microphenocrysts (in decreasing order of abundance) and accessory opaque microphenocrysts (SMFig. 1a). In addition to occurring as well formed, euhedral pheno- and microphenocrysts both plagioclase and olivine occur occasionally as larger anhedral crystals (respectively 5-6 mm and ~1 mm). Glomerules of plagioclase, clinopyroxene and opaques (±olivine) are locally found.

A second type of 1902-03 scoria (e.g. SVG42, 44 and 72) shows a mafic-rich mineralogy characterized by plagioclase and clinopyroxene phenocrysts in similar quantities (~1 mm in length on average, with larger crystals up to ~2 mm) together with olivine, occasionally found as polymineralic aggregates (SMFig. 1c). Opaque oxides occur only as inclusions within clinopyroxene and olivine. The glassy groundmass displays local portions of high vesicularity with sparse microphenocrysts of plagioclase, clinopyroxene, olivine, orthopyroxene and opaque oxides set within a light brown glassy matrix, possibly suggesting mingling with some compositionally different magma batches.

The other eruptions described show a similar petrography - see Table 2 for details.

sample	Eruption	Pl	Cpx	Opx	Ol	Op	texture	notes
SVG42	1902-03 (mafic-rich scoria)	XXX	XXX		X		strongly porphyritic, weakly vesicular; glassy groundmass	Cpx-rich enclave
SVG44		XXX	XXX		X		strongly porphyritic, moderately vesicular; glassy groundmass	light brown glass patches with higher vesicularity and crystals of Pl, Cpx, Ol, Opx and Op; dunitic enclave
SVG72		XXX	XXX		XX		strongly porphyritic, moderately vesicular; glassy groundmass	Ol+Cpx and micro-gabbroic enclaves
SVG24	1902-03	XXX	XX	X	tr	tr	moderately porphyritic, (relatively) fine-grained, weakly vesicular; dusty groundmass	Amph+Pl+Cpx enclave
SVG28		XXXX	XX	X	tr	tr	strongly porphyritic, (relatively) fine-grained, moderately vesicular; glassy groundmass	
SVG14		XXXX	XX	x	x	x	strongly porphyritic + glomeroporphyritic, weakly vesicular; glassy groundmass	big green/brown Amph; common anhedral Pl
SVG3	1718-1812	XXXX	XX	x	tr	x	strongly porphyritic, weakly vesicular; glassy groundmass	
SVG16		XXX	XX	x	tr	x	strongly porphyritic + glomeroporphyritic, moderately vesicular; glassy groundmass	troctolitic enclave
SVG1	1580	XXXX	XX	x	tr	tr	strongly porphyritic + glomeroporphyritic, weakly vesicular; glassy groundmass	lava (Pl+Cpx) lithic; light brown glass patches with higher vesicularity
SVG4		XXXX	XX	X	tr	tr	strongly porphyritic + glomeroporphyritic, weakly vesicular; glassy groundmass	Ol-gabbroic enclave
SVG50		XXXX	XX	x		tr	strongly porphyritic + glomeroporphyritic, moderately vesicular; glassy groundmass	

SVG60	1440	XXX	XX	X	tr	tr	strongly porphyritic + glomeroporphyritic, moderately/weakly vesicular; dusty groundmass	micro-noritic enclave
SVG61		XXXX	XX	X	x	tr	strongly porphyritic + glomeroporphyritic, weakly vesicular; glassy groundmass	
SVG62		XXXX	XX	X	tr	tr	moderately porphyritic + glomeroporphyritic, moderately vesicular; dusty groundmass	
SVG63		XXXX	XX	x	x	tr	strongly porphyritic + glomeroporphyritic, moderately vesicular; dusty glassy groundmass	
XXXX = dominant, XXX = very common, XX = quite abundant, X = not very abundant, x = few crystals, tr = traces								

Table 2 Summary of the main petrographic features of the collected scoria samples from the investigated historical and prehistorical eruptions of the La Soufrière volcano. Pl = plagioclase; Cpx = clinopyroxene; Opx = orthopyroxene; Ol = olivine; Op = opaque minerals; Amph = amphibole.

7.2 Mineral and glass chemistry

Plagioclase. Phenocrysts of plagioclase from all studied eruptions display a wide compositional range from labradorite/andesine to bytownite/anorthite (i.e. $An_{49-96}Ab_{5-50}Or_{0-2}$), with no systematic core to rim compositional differences, although single crystals commonly show a normal zoning. Occasional anhedral plagioclase from the 1902-03 scoria (SMFig. 1b) generally falls in the An-richer end of the above compositional spectrum (i.e. $An_{72-95}Ab_{4-28}Or_{0-1}$). Plagioclase inclusions in olivine, clinopyroxene, orthopyroxene are broadly homogeneous, possibly suggesting a contemporaneous segregation.

Clinopyroxene. A notably Ti-poor (Ti < 0.051 apfu) clinopyroxene is the main ferromagnesian phase of all the investigated samples, covering a wide range from (mainly aluminian, i.e., Al > 0.1 apfu; Morimoto, 1988) diopside to augite. In scoria from the historical eruptions, clinopyroxene is mostly augitic and covers the range $Wo_{35-45}En_{40-46}Fs_{13-20}$ [Mg# = Mg# = molar $Mg/(Mg+Fe^{2+})$ = 0.69-0.78]. A core to rim decrease of Mg# (from 0.71-0.77 to 0.70-0.72), coupled with Ca decrease (from 0.763-0.829 to 0.692-0.816 apfu), is evident only for 1718-1812 clinopyroxene. Less abundant diopsidic clinopyroxene is present mainly in the 1902-03 mafic-rich scoria crystal cores ($Wo_{45-51}En_{39-44}Fs_{8-13}$, Mg# = 0.76-0.84).

Some anhedral clinopyroxene found in the 1902-03 mafic-rich scoria have remarkably Mg-rich aluminian diopsidic cores ($Wo_{46-50}En_{42-47}Fs_{6-9}$, Al = 0.127-0.304 apfu, Mg# = 0.83-0.88) surrounded by Mg-poorer aluminium diopsidic/augitic rims ($Wo_{44-45}En_{41-43}Fs_{13-14}$, Al = 0.132-0.195 apfu, Mg# = 0.74-0.78). Clinopyroxene from the prehistoric eruptions is generally more homogeneous (mostly augite,

517 with some sporadic diopside) and poorer in Mg (Mg# = 0.69-0.77) and Al (generally in the 0.060-0.126
518 apfu range, occasionally up to 0.220 apfu) with respect to that from the historical activity.
519
520 *Olivine*. A relatively abundant phenocryst phase only in the mafic-rich 1902-03 scoria samples,
521 characterized by a quite large compositional variation (Mg# = 0.71-0.86, with crystal cores being
522 generally Mg-richer). The fewer olivine phenocrysts/microphenocrysts analysed in the remaining
523 samples are generally more homogeneous and Mg-poorer, covering the Mg# range of 0.63-0.77.
524 Anhedral olivine crystals from the historical eruptions display slightly Mg-richer compositions with
525 respect to phenocryst phases for both the 1902-03 (Mg# = 0.74-0.79 vs. 0.63-0.76) and the 1902/03
526 mafic-rich scoria (Mg# = 0.72-0.88, typically normally zoned). Within 1718-1812 scoria the large
527 anhedral, occasionally rounded, olivine is significantly Mg-poorer, with Mg# = 0.65-0.76.
528
529 *Orthopyroxene*. A typical mineral phase in scoria in most eruptions, whereas it occurs only as
530 inclusions (Mg# = 0.65-0.71) within clinopyroxene phenocrysts in the 1902-03 mafic scoria.
531 Compositions are quite constant in all the analysed samples, with Mg concentrations being slightly
532 higher in the scoria from the 1902-03 (Mg# = 0.65-0.72) and 1718-1812 historical eruptions (Mg# =
533 0.64-0.70), with respect to those from the 1580 (Mg# = 0.63-0.67) and 1440 (Mg# = 0.63-0.68).
534
535 *Opaque minerals*. The main opaque mineral is Ti-magnetite, diffusely found as a
536 microphenocryst/microcryst in all but the 1902-03 mafic-rich samples. Compositions are basically
537 constant, mostly with Usp (ulvöspinel mol.%) and Mg# respectively in the ranges of ~30-40 mol.% and
538 0.09-0.12.
539
540 *Glass*. Analysed groundmass glass covers a notably wide compositional range. Although this might at
541 least in part reflect the variable crystallinity of the analysed samples, an overall increase in the degree
542 of evolution can be observed moving from basaltic andesite and andesite in the 1902-03 mafic-rich
543 scoria (SiO_2 = 56.6-62.6 wt.%; Mg# = 0.19-0.46), to dacite in the 1902-03 (SiO_2 = 64.4 wt.%, Mg# =
544 0.17), to andesite/dacite in the 1718-1812 (SiO_2 = 60.8-68.0 wt.%, Mg# = 0.21-0.34), dacite in the 1580
545 (SiO_2 = 64.4-65.9 wt.%, Mg# = 0.28-0.36) and 1440 samples (SiO_2 = 60.1-68.7 wt.%, Mg# = 0.12-0.27).
546 Glass inclusions in the main phenocryst phases, especially in plagioclase and clinopyroxene, basically
547 show similar chemical trends.
548
549 **7.4 Whole-rock geochemistry**

Scoria analysed show a relatively limited compositional range in terms of Total Alkalis vs. Silica (TAS; Fig. 6a), ranging from basalts (mainly represented by 1902-03 mafic-rich scoria samples) to more abundant basaltic andesites. Samples from the 1902-03 eruption show the greatest compositional variability (i.e., SiO_2 = 50.2-54.8 wt.%), with the mafic-rich scoria at the least evolved end. Samples from the 1718-1812 eruption also show some compositional variability, mainly overlapping with that of the 1902-03 eruption but also including slightly more evolved compositions (SiO_2 = 53.7-55.9 wt.%). Scoria from the prehistoric eruptions are generally notably homogeneous and more evolved (i.e., SiO_2 = 55.3-56.4 and 55.2-56.7 wt.%, respectively for 1580 and 1440).

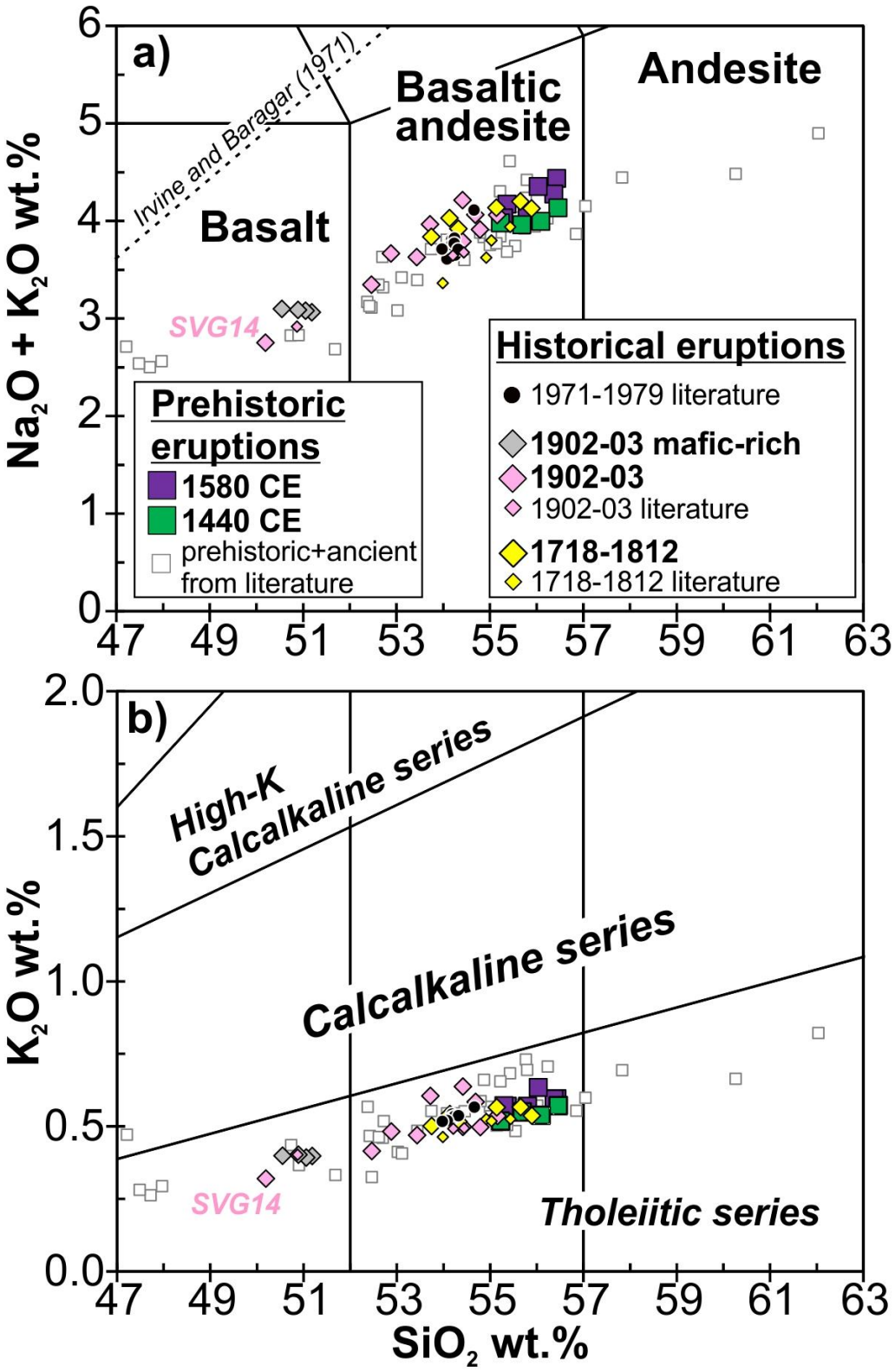

Fig 6 a) TAS (Total Alkali vs. Silica; LeMaitre, 2002) and b) K_2O vs. SiO_2 (Le Maitre, 2002) diagrams for the analysed La Soufrière juvenile samples. Sample SVG14 (1902-03) showing some anomalous chemical features is highlighted (see text). Also shown are the literature data for the prehistoric and ancient activity (Heath et al., 1998) and 1971-79 eruptions (Graham and Thirlwall, 1981). In a) the dashed line separates the fields for subalkaline and alkaline rock series (Irvine and Baragar, 1971).

Our samples fall well within the entire La Soufrière compositional field, which ranges from more primitive basaltic (i.e., SiO_2 = 47.2-48.0 wt.%) to more evolved andesitic compositions (SiO_2 = 57.8-62.3 wt.%) among the products of the prehistoric and ancient activity. Overall, the La Soufrière samples depict a quite linear trend for a clearly subalkaline rock series with low-K tholeiitic affinity (Fig. 6b). Although a detailed discussion on such topics is out of the scope of this paper, the serial affinity of the products of the La Soufrière (as well as of those of the Lesser Antilles volcanism in general) has been debated by a number of authors (e.g., Smith et al. 1996; Heath et al. 1998; Macdonald et al. 2000 and references therein), and either tholeiitic, calcalkaline or transitional affinities have been proposed. In any case, it is of note that our data is perfectly in line with published data.

Harker-type binary variation diagrams (Fig. 7) depict quite linear differentiation trends, moving from the 1902-03 mafic-rich scoria to the products of the prehistoric eruptions. With the only exception of a single 1902-03 scoria sample (SVG14), a general decrease of MgO, CaO, Sc, Ni and Cr and an increase of SiO_2, Na_2O, K_2O, Ba, Y, Zr seem to characterize the differentiation of the investigated La Soufrière samples. In addition, both Al_2O_3 (first increasing and then decreasing) and Sc (first remaining constant, then rapidly decreasing) experience an evident discontinuity in their differentiation trends at SiO_2 ~52 wt.%. This is consistent with both petrography and mineral (and glass) phases chemical variations, as well as with the overall literature for La Soufrière samples.

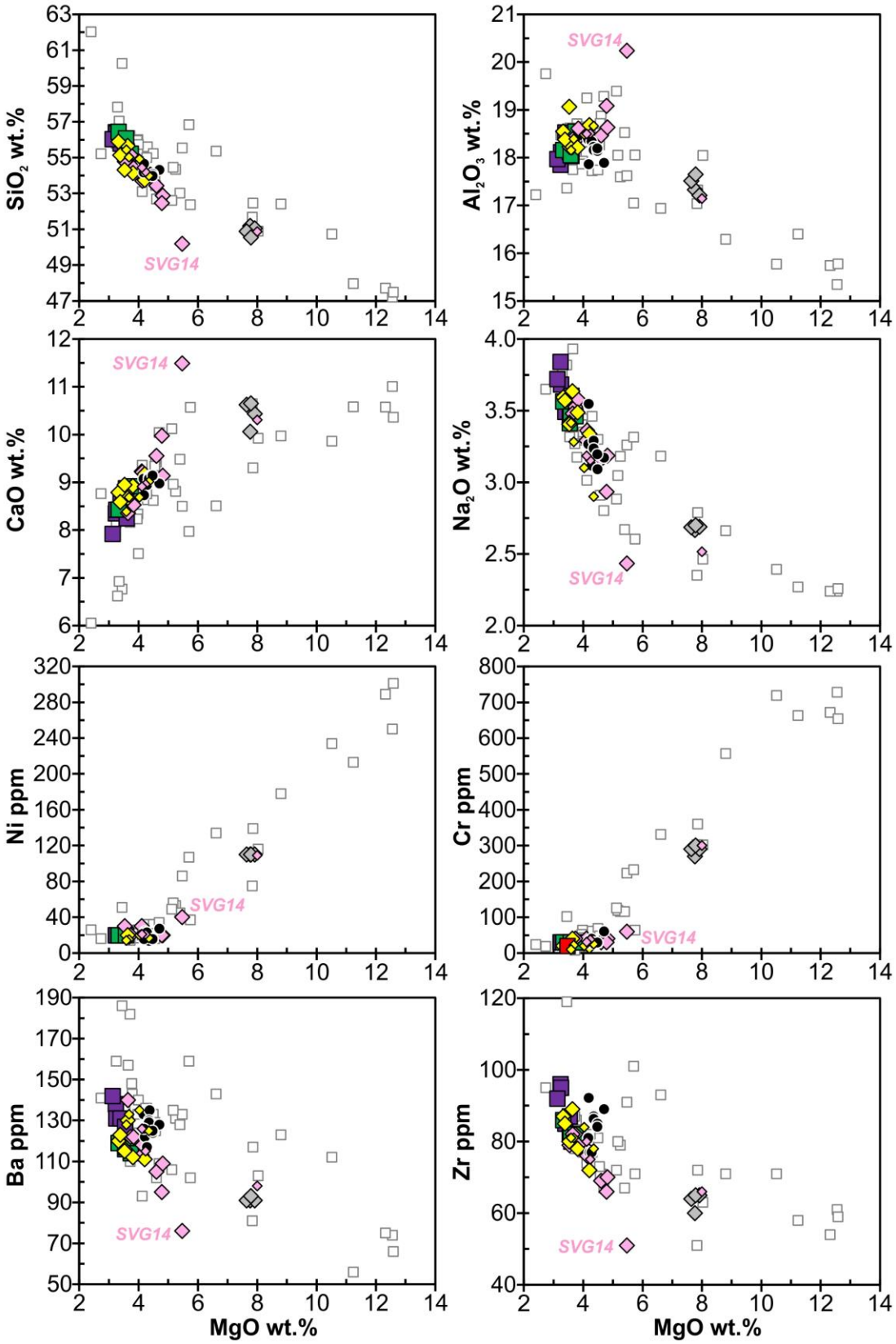

585

586 **Fig 7** Selected major- and trace element binary variation diagrams for the analysed La Soufrière
587 juvenile samples. Sample SVG14 (1902-03) showing some anomalous chemical features is highlighted
588 (see text). Symbols and literature data as in Fig. 7.

589

8. Discussion

8.1 Eruption Frequency and style

Radiocarbon dating has allowed identification of two prehistoric eruptions that have occurred in the last 1000 years at La Soufrière St Vincent. One in the 16th century with a mean calibrated age of 1580 CE (based on six dates), and another in the 15th Century with a mean calibrated age of 1440 CE (three dates). Owing to the nature of the radiocarbon calibration curve together with a paucity of distinctive features, it is difficult to separate the deposits of the 1718 and 1812 eruptions. Indeed, it is possible that the eruption in 1718 generated limited PDCs and thus the studied deposits represent mainly the 1812 eruption.

Our radiocarbon dating shows that over the last 1000 years there were at least six explosive eruptions with a repose period varying between 77 and ~140 years, This gives a mean periodicity of 90 years between explosive eruptions from 1440 until 1979.

It is clear however that the repose period between eruptions has not remained constant with time. A notable decrease in repose times is evident: > 300 yr before 1440 CE (although with large uncertainty), 140 yr before 1580 CE, 138 yr before 1718, 96 yr before 1812, 90 yr before 1902-03 and 77 yr before 1979. This might indicate that a future eruption could be < 77 years since 1979, giving rise to the possibility of an explosive eruption before 2059 if this trend were to continue, although this is associated with a very large uncertainty and of course the volcano might not follow the same pattern. The effusive activity which occurred in 1971 is not considered here, furthermore there is the possibility of an effusive dome forming eruption around 1784 and others that may have not been recorded. Including these effusive events would result in a different pattern of activity not considered here.

Almost all the eruptions generated PDCs and in most cases numerous PDCs travelled down valleys draining the southern and lowest part of the crater. Most of these PDCs deposits were scoria flows (frequently referred to as 'Soufrière type', McBirney and Williams 1979) considered to have been generated by collapse of eruption columns, as was originally proposed for the 1902 events by Hay (1958). However evidence indicates that each eruption was quite different in terms of the magnitude, initial ash-rich activity e.g. 1902, 1812 CE eruptions, or magmatic 'plinian type' lapilli fallout 1580 CE. In addition PDC deposits at the base of the 1440 CE eruption do not contain vesicular scoria and may have involved collapse of lava domes to generate block and ash flow types PDCs, indeed lapilli fallout containing abundant dense, poorly vesicular clasts suggest powerful Vulcanian explosions associated with destruction of such lava domes. Thus apart from Scoria-rich 'Soufrière type' PDCs which were involved with most eruptions, each event varied significantly.

623

624 The distribution of the products formed by eruptions in the last 1000 years indicates that the pre-
625 existing topography of the volcanic edifice has had a considerable effect on them. No products
626 formed in the last 1000 years crop out on the northern and eastern flanks. However, extensive
627 knowledge of the 1902 eruption demonstrates that dilute, low-concentration PDCs capable of
628 causing extensive fatalities travelled down the northern and eastern flanks. This highlights the
629 danger of using preserved geology in hazard analysis. Preservation of products from such activity is
630 extremely poor, particularly so on the steep flanks of a tropical volcano.

631 Most historical explosive activity was associated with abundant ashfall that extended to other
632 islands. Evidence indicates some of the initial 1902 activity was phreatomagmatic and the initial
633 1812 activity was also ash-rich. The presence of a crater lake prior to both these eruptions possibly
634 played an important role in this. The basal fallout sequence of the 1902-03 eruption also preserves
635 evidence of more intermittent explosive Vulcanian type activity. However, significant lapilli fallout
636 formed by considerable convecting eruption columns were only associated with the prehistoric
637 eruptions (1440 and 1580 CE).

638 The 1580 CE PDC deposits form a large part of the fans in and around the main valleys draining the
639 crater, in particular in the SW in coastal sections. These deposits form some of the thickest and most
640 widespread products of the last 1000 years, indicating that this eruption was potentially the largest
641 in the last 1000 years.

642

643 ***8.2 Petrochemical implications***

644 The petrochemical characterization has revealed a relatively limited compositional variation of the
645 magmas feeding the most recent prehistoric and historical eruptions. Our new data are consistent
646 with the few available literature counterparts, and fall well within the wider compositional spectrum
647 defined by the dataset for the entire history of La Soufrière's activity. Chemical trends are quite
648 linear, suggesting a genetic relationship linking the most evolved products of the 1440 and 1580 CE
649 prehistoric eruptions with the progressively less evolved products of the 1718-1812 and 1902-03
650 historical eruptions. It could be proposed that the more evolved compositions of both the
651 prehistoric eruptions might have led to retention of volatiles and thus a more violent explosive
652 nature (consistent with the stratigraphic data for the 1580 CE eruption; see previous paragraph).

653 It seems likely that magma evolution was substantially driven by crystal fractionation firstly involving
654 mainly olivine, clinopyroxene and plagioclase (i.e., decreasing MgO, CaO, Ni, Cr, increasing Al_2O_3, and

alkalis) and then plagioclase, clinopyroxene, orthopyroxene and Fe-Ti oxides (decreasing Al_2O_3, Fe_2O_3tot and V at MgO <4 wt.%). This is in line with the petrographic features of the two recognized scoria types, as well as with the chemical trends of the analysed mineral and glass phases (see "Petrography" and "Mineral and glass chemistry" sections).

Notably deviating is the composition of 1902-03 scoria sample SVG14, featuring the lowest SiO_2 coupled with unusually high Al_2O_3 (20.2 wt.%), CaO (11.5 wt.%) and Sr (232 ppm), and low MgO (5.47 wt.%), Sc (31 ppm), Ni (40 ppm) and Cr (60 ppm). Given the overall similarity in petrography and mineral and glass chemistry of such sample with all the other 1902-03 scoria samples, and the typical presence of notably An-rich anhedral plagioclase (up to An_{96}; Fig. 6b), it seems likely that the composition of this sample has been significantly modified by plagioclase cumulation. This testifies to a limited additional role played by open-system processes (e.g., magma mixing, assimilation of crystal mushes), which is plausible, given the common presence of cumulate-textured enclaves, in the lava and pyroclasts of the La Soufrière volcano (e.g., Heath et al. 1998; Tollan et al. 2012), as well the gabbroic to ultramafic enclaves reported for the investigated scoria samples (see "Petrography" section and Table 2).

The paramount role of crystal fractionation in the evolution of La Soufrière magma has been long recognised by both whole-rock and mineral petrochemical studies (Heath et al., 1998), and thorough experimental work at various P and H_2O content conditions (Pichavant et al., 2002; Pichavant and Macdonald, 2007; Melekhova et al., 2015). Although the existence of four (slightly) different magma lineages related with differences in P (from 1.3 to < 0.4 GPa) and H_2O contents (2.3-4.5 wt.%) of the parental magmas (plus occasional partial melting of water-poor high-MgO basalt that solidified at depth; Melekhova et al., 2015) has been proposed, no attempt has been made to link these to a specific periods of the volcanic history.

The possible existence of time-related trends in the composition of the magmas erupted at La Soufrière can be thus only crudely evaluated through simple chemostratigraphic investigation. Older sequences of the volcano ranging up to 600 ka (Figs. 6 and 7) show a much wider chemical variation than the eruptions in the last 600 years reported here. In fact, the most recent products show the narrowest range of composition in the volcano's history. Further detailed study is required, possibly allowing a better evaluation of the geochemical vertical trends within the deposits of a single eruption (only occasionally and crudely evaluated here for stratigraphic sections showing the most favourable exposure conditions; Figs. 4 and 5). However, what can be tentatively suggested at this stage is that in the more recent history, magma might have more readily found the opportunity to evolve and homogenise within shallow reservoirs eruption of relatively primitive basaltic magmas

688 occurred only rarely, as in the 1902-03 (possibly being evidence of magma chamber rejuvenation
689 acting as eruption trigger).

690

691 **9. Conclusions**

692 • The period of the last 600 years at La Soufrière St Vincent has involved six explosive
693 eruptions with repose periods of 77 and ~140 years. There is a decrease in the repose period
694 between explosive eruptions with time, with the shortest repose period between the most
695 recent explosive eruptions in 1902 and 1979

696

697 • Deposits formed are predominantly 'scoria flow type' PDCs formed by collapse of eruption
698 columns, although some block and ash flow type PDCs, associated with the collapse of lava
699 domes, were formed during the 1440 CE eruption

700

701 • Only the prehistoric eruptions in 1440 and 1580 CE, were associated significant lapilli fallout
702 deposits. These events were the most evolved geochemically with slightly higher SiO_2 values
703 than the historical events.

704

705 • Initial activity associated with the 1902-03 and 1812 eruption was ash-rich and, certainly for
706 1902, the products were rich in lithic material and accretionary lapilli. These features suggest
707 that the initial events of these eruptions were phreatomagmatic.

708

709 • Despite the paroxysmal PDCs formed on 7th May 1902 being spread largely radially around
710 the volcano, remnants of deposits are only preserved to the southwest and southeast,
711 highlighting the incomplete and unreliable nature of spatial extent, based on geologically
712 preserved products, for hazard analysis.

713

714 • Erupted basalt-basaltic andesite magmas are generally less variable in the last 600 years
715 with respect to the ancient phase of La Soufrière's activity. This possibly suggests that the
716 feeding magmatic system has attained the conditions for effective magma homogenisation
717 through fractional crystallisation (plus occasional open-system processes), only sporadically
718 allowing the emplacement of relatively primitive terms.

719

Acknowledgements

Lara Mani is thanked for assistance in the field, particularly on the initial visit to the Larikai. Jack Palmer for help with initial geochemical work. The authors wish to thank Roberto De Gennaro for skilled help during EDS microanalyses. Some of the radiocarbon dating in this work was supported by the NERC Radiocarbon Facility NRCF010001 (allocation number 1845.1014). Fieldwork for this work was supported by the UK Natural Environment Research Council (NERC) and Economic and Social Research Council (ESRC) through the Increasing Resilience to Natural Hazards programme [STREVA project, Grant numbers NE/J020001/1. We thank David Pyle and Patrick Bachelery for constructive reviews that improved this manuscript.

References

Anderson and Yonge 1785 An account of Morne Garou, a Mountain on the island of St Vincent, with a description of the volcano on its summit. Phil Trans R Soc London 75:16-31

Anderson, T., 1908. Report on the Eruption of the La Soufrière in St. Vincent, in 1902, and a Visit to Montagne Pelée in Martinique, Part II, the Change in the Districts and the Subsequent history of the Volcanoes. Phil. Trans. R. Soc. A 208, 275–303.

Anderson, T., Flett, J.S., 1903. Report on the Eruptions of the La Soufrière in St. Vincent, in 1902, and on a Visit to Montagne Pelée in Martinique, Part I. Phil. Trans. R. Soc. A 200, 353–553.

Aspinall, W.P., Sigurdsson, H., Shepherd, J.B., 1973. Eruption of Soufriere Volcano on St Vincent Island. 1971-1972. Science 181, 117 124.

Blue Book, 1902. Correspondence relating to the volcanic eruptions in St Vincent and Martinique in May 1902, with map and appendix: Parliamentary Paper by Command, Cd. 1201, HMSO, London.

Brazier, S., Davis, A.N., Sigurdsson, H., Sparks, R.S.J., 1982. Fallout and deposition of Volcanic ash during the 1979 explosive eruption of the La Soufrière St Vincent. J. Volcanol. Geotherm. Res. 14, 335-359.

Briden, J.C., Rex, D.C., Faller, A.M., Tomblin, J.F., 1979. K-Ar geochronology and palaeomagnetism of volcanic rocks in the Lesser Antilles island arc. Phil. Trans. R. Soc. A 291, 485-528.

Bronk Ramsey, C., 2009. Bayesian analysis of radiocarbon dates. Radiocarbon 51, 337-360.

Defoe D (1718) An account of the island of St Vincent in the West Indies and of its entire destruction

on 26th March last, with some rational suggestions concerning the causes and manner of it. Mists Weekly J, issues 82, July 5.

DeMets, C., Jansma, P.E., Mattioli, G.S., Dixon, T.H., Farina, F., Bilham, R., Calais, E., Mann, P., 2000. GPS geodetic constraints on Caribbean-North America Plate Motion. Geophys. Res. Lett. 27, 437-440.

Fournier, N., Moreau, M., Robertson, R., 2011. Disappearance of a crater lake: implications for potential explosivity at La Soufrière volcano, St Vincent, Lesser Antilles. Bull. Volcanol. 73, 543-555.

Graham, A.M., Thirlwall, M.F., 1981. Petrology of the 1979 eruption of La Soufrière Volcano, St. Vincent, Lesser Antilles. Contrib. Mineral. Petrol. 76, 336-342.

Hay, R.L., 1959. Formation of the Crystal-Rich Glowing Avalanche Deposits of St. Vincent, B.W.I. J. Geol. 67, 540-562.

Heath, E., 1997. Genesis and evolution of calc-alkaline magmas at Soufrière volcano, St. Vincent, Lesser Antilles arc. Unpublished PhD Thesis, University of Lancaster.

Heath, E., MacDonald, R., Belkin, H., Hawkesworth, C., Sigurdsson, H., 1998. Magmagenesis at La Soufrière Volcano, St Vincent, Lesser Antilles Arc. J. Petrol. 39, 1721-1764.

Hovey, E.O., 1903. Martinique and St. Vincent; a Preliminary Report upon the Eruptions of 1902. Bull. Am. Mus. Nat. Hist. 16, 333–372.

Irvine, T., Baragar,W., 1971. A guide to the chemical classification of the common volcanic rocks. Can. J. Earth Sci. 8, 523-548.

Lamb, O., Varley, N.R., Mather, T.A., Pyle, D.M., Smith, P.J., Liu, E.J., 2014. Multiple timescales of cyclical behavior observed at two dome-forming eruptions. J. Volcanol. Geotherm. Res. 284, 106-121.

Le Friant, A., Boudon, G., Arnulf, A., Robertson, R.E.A., 2009. Debris avalanche deposits offshore St. Vincent (West Indies): Impact of flank-collapse events on the morphological evolution of the island. J. Volcanol. Geotherm. Res. 179, 1-10.

Le Maitre, R.W., 2002. Igneous Rocks: A Classification and Glossary of Terms. Recommendations of the International Union of Geological Sciences Subcommission on the Systematics of Igneous Rocks. Cambridge University Press, Cambridge, UK, 256 pp.

Luhr, J.F., Carmichael, I.S.E., 1990. Petrological monitoring of cyclical eruptive activity at Volcán Colima, Mexico. J. Volcanol. Geotherm. Res. 42, 235-260.

McBirney, H., Williams, A.R., 1979. Volcanology. Freeman, Cooper & Co, 400 pp.

Macdonald, R., Hawkesworth, C., Heath, E., 2000. The Lesser Antilles volcanic chain: a study in arc magmatism. Earth-Sci. Rev. 49, 1-76.

Melekhova, E., Blundy, J., Robertson, R., Humphreys, M.C.S., 2015. Experimental evidence for polybaric differentiation of primitive arc basalt beneath St. Vincent, Lesser Antilles. J. Petrol. 56, 161-192.

Morimoto, N., 1988. Nomenclature of pyroxenes. Mineral. Petrol. 39, 55-76.

Odbert, H.M., Stewart, R.C., Wadge, G., 2014. Chapter 2 - Cyclic phenomena at the La Soufrière Hills Volcano, Montserrat. In: Wadge, G., Robertson, R.E.A., Voight, B. (eds.), The Eruption of Soufrière Hills Volcano, Montserrat from 2000 to 2010. Geological Society, London, Memoirs 39, 41-60. doi: 10.1144/M39.2

Pichavant, M, Macdonald, R., 2007. Crystallization of primitive basaltic magmas at crustal pressures and genesis of the calc-alkaline igneous suite: experimental evidence from St. Vincent, Lesser Antilles arc. Contrib. Mineral. Petrol. 154, 535-558.

Pichavant, M., Mysen, B.O., Macdonald, R., 2002. Source and H_2O content of high-MgO magmas in island arc settings: an experimental study of primitive calc-alkaline basalt from St. Vincent, Lesser Antilles arc. Geochim. Cosmochim. Acta 66, 2193-2209.

Pindell, J.L., Cande, S.C., Pitman III, W.C., Rowley, D.B., Dewey, J.F., LaBrecque, J., Haxby, W., 1988. A plate-kinematic framework for models of Caribbean evolution. Tectonophysics 155, 121-138.

Pyle, D.M., Barclay, J., Armijos, M.T., 2018. The 1902–3 eruptions of the Soufrière, St Vincent: Impacts, relief and response. J. Volcanol. Geotherm. Res. 356, 183-199.

Robertson, R.E.A., 1992. Volcanic hazard and risk assessment of the La Soufrière volcano, St. Vincent, West Indies. Unpublished MPhil thesis.

Robertson, R.E.A., 2005 St Vincent. In: Lindsay, J., Robertson, R., Shepherd, J., Ali, S. (eds.), Volcanic Hazard Atlas of the Lesser Antilles.

Roobol, M.J., Smith, A.L., 1975. A comparison of the recent eruptions of Mt. Pelée, Martinique and La Soufrière, St. Vincent. Bull. Volcanol. 39, 214-240.

Rowley, K., 1978a. Stratigraphy and geochemistry of the Soufriere volcano, St. Vincent WI. Unpublished PhD thesis.

809 Rowley, K., 1978b. Late Pleistocene pyroclastic deposits of Soufrière Volcano, St. Vincent, West Indies.
810 Geol. Soc. Am. Bull. 6, 825-835.

811 Shepherd, C., 1831. An historical account of the island of Saint Vincent. Nicol, London, 216 pp.

812 Shepherd, J.B., Sigurdsson, H., 1982. Mechanism of the 1979 explosive eruption of soufriere volcano,
813 St. Vincent. J. Volcanol. Geotherm. Res. 13, 119-130.

814 Shepherd, J.B., Aspinall, W.P., Rowley, K.C., Pereira, J., Sigurdsson, H., Fiske, R.S., Tomblin, J.F., 1979.
815 The eruption of Soufriere volcano, St. Vincent, April-June 1979. Nature 282, 24-28.

816 Smith, S.D., 2011, Volcanic hazard in a slave society: the 1812 eruption of Mount La Soufrière in St
817 Vincent. J. Hist. Geogr. 37, 55-67.

818 Smith, T.E., Thirlwall, M.F., Macpherson, C., 1996. Trace element and isotope geochemistry of the
819 volcanic rocks of Bequia, Grenadine Islands, Lesser Antilles Arc: a study of subduction enrichment
820 and intra-crustal contamination. J. Petrol. 37, 117-143.

821 Sparks, R.S.J., Aspinall, W.P., 2004. Volcanic activity: frontiers and challenges in forecasting, prediction
822 and risk assessment. In: Sparks, R.S.J., Hawkesworth, C.J. (eds.), The state of the planet: frontiers
823 and challenges in geophysics. Washington, DC: American Geophysical Union, pp. 359-373.
824 doi:10.1029/150GM28

825 Stuiver, M., Reimer, P.J., and Reimer, R.W., 2018. CALIB 7.1 [WWW program] at http://calib.org,
826 accessed 2018-7-9

827 Tollan, P.M.E., Bindeman, I., Blundy, J.D., 2012. Cumulate xenoliths from St. Vincent, Lesser Antilles
828 Island Arc: a window into upper crustal differentiation of mantle-derived basalts. Contrib. Mineral.
829 Petrol. 163, 189-208.

830

831

832

833 **Electronic Supplementary Material 1** Representative whole-rock, mineral chemistry and glass
834 composition data for the analysed scoria samples from the 1440 CE, 1580 CE, 1718-1812 and 1902-
835 03 eruptions of the La Soufrière volcano.

836 **Table SM1** Representative major element concentrations (wt.%) and calculated structural formulae
837 (apfu, atoms per formula unit, on 6 oxygens and 4 cations) for clinopyroxene (cpx) and
838 orthopyroxene (opx) crystals from the analysed scoria samples from the 1440 CE, 1580 CE, 1718-

839 1812 and 1902-03 eruptions of the La Soufrière volcano.
840 * = mafic-rich scoria
841 bdl = below detection limits
842 Mg# = Mg/(Mg+Fe^{2+}); En = enstatite mol.%; Wo = wollastonite mol.%; Fs = ferrosilite mol.%
843 cpx-anh = anhedral cpx; mpc = microphenocryst

844

845 **Table SM2** Representative major element concentrations (wt.%) and calculated structural formulae
846 (apfu, atoms per formula unit, on 8 oxygens and 5 cations) for plagioclase crystals (pl) from the
847 analysed scoria samples from the 1440 CE, 1580 CE, 1718-1812 and 1902-03 eruptions of the La
848 Soufrière volcano.
849 * = mafic-rich scoria
850 bdl = below detection limits
851 Ab = albite mol.%; Or = orthoclase mol.%; An = anorthite mol.%
852 pl-anh = anhedral pl; mpc = microphenocryst

853

854 **Table SM3** Representative major element concentrations (wt.%) and calculated structural formulae
855 (apfu, atoms per formula unit) for olivine crystals (ol, on 4 oxygens and 3 cations) from the analysed
856 scoria samples from the 1440 CE, 1718-1812 and 1902-03 eruptions of the La Soufrière volcano.
857 * = mafic-rich scoria
858 bdl = below detection limits
859 Mg# = Mg/(Mg+Fe^{2+}); Fo = forsterite mol.%; Fa = fayalite mol.%; Teph = tephroite mol.%
860 ol-anh = anhedral ol; mpc = microphenocryst

861

862 **Table SM4** Representative major element concentrations (wt.%) and calculated structural formulae
863 (apfu, atoms per formula unit) for Ti-magnetite crystals (mt, on 4 oxygens and 3 cations) from the
864 analysed scoria samples from the 1440 CE, 1580 CE, 1718-1812 and 1902-03 eruptions of the La
865 Soufrière volcano.
866 * = mafic-rich scoria
867 bdl = below detection limits
868 Ulvöspinel mol% (Usp%), and FeO and Fe_2O_3 were calculated following Carmichael (1967)
869 Mg# = Mg/(Mg+Fe^{2+}); Cr# = Cr/(Cr+Al)

mpc = microphenocryst; in ol = inclusion in olivine; in cpx = inclusion in clinopyroxene; in opx = inclusion in orthopyroxene

Table SM5 Representative major element concentrations (wt.%) for groundmass glass from the analysed scoria samples from the 1440 CE, 1580 CE, 1718-1812 and 1902-03 eruptions of the La Soufrière volcano.
* = mafic-rich scoria
bdl = below detection limits
Mg# = $Mg/(Mg+Fe^{2+})$
gm = groundmass; in ol = inclusion in olivine; in cpx = inclusion in clinopyroxene; in pl = inclusion in plagioclase; in opx = inclusion in orthopyroxene

Table SM6 Major- and trace element concentrations (respectively in wt.% recalculated to 100% on a water-free basis, and in ppm) for the analysed scoria samples from the 1440 CE, 1580 CE, 1718-1812 and 1902-03 eruptions of the La Soufrière volcano.
* = mafic-rich scoria
bdl = below detection limits
Mg# = molar $Mg/(Mg+Mn+Fe^{2+})$

Figure SM1